

Biofilm formation, antibiotic resistance, and genome sequencing of a unique isolate *Salmonella* Typhimurium M3

Lei Yuan^{1,2}, Yang Liu¹, Luyao Fan¹, Caowei Chen¹, Zhenquan Yang^{1*}, Xin-an Jiao^{2*}

¹College of Food Science and Engineering, Yangzhou University, Yangzhou, PR China; ²Jiangsu Key Laboratory of Zoonoses, Yangzhou, PR China

***Corresponding authors:** Zhenquan Yang, Yangzhou University, 196 Huayang West Road, Yangzhou, Jiangsu 225127, PR China. Email: yangzq@yzu.edu.cn; Xinan Jiao, Jiangsu Key Laboratory of Zoonoses, Yangzhou, Jiangsu, 225009, PR China. Email: jiao@yzu.edu.cn

Received: 19 October 2022; Accepted: 4 January 2023; Published: 13 January 2023

© 2023 Codon Publications



RESEARCH ARTICLE

Abstract

Salmonella Typhimurium is a zoonotic bacterium that can cause salmonellosis, and the major concerns of *S. Typhimurium* for the food industry are its ability to obtain multidrug resistance and form biofilms on food-contact surfaces. In the current study, the antimicrobial resistance of a strong biofilm former *S. Typhimurium* M3 was assessed by the diffusion method. Genome sequencing was also applied to obtain the genes related to antibiotic resistance, and biofilm formation of *S. Typhimurium* M3. Biofilm-forming capacity of *S. Typhimurium* M3 was found to be strain dependent, and a high number of isolates were strong biofilm formers. The high biofilm-forming isolate *S. Typhimurium* M3 was resistant to oxacillin, lincomycin, rifampicin, tetracycline, and clindamycin, with the MIC values of 512 µg/mL, 32 µg/mL, 16 µg/mL, 64 µg/mL, and 64 µg/mL, respectively. Genomic annotation of *S. Typhimurium* M3 showed the presence of genes involved in cellulose biosynthesis, curli production, fimbriae biosynthesis, flagellar assemble, quorum sensing, chemotaxis, and some transcriptional regulators. Antibiotic efflux conferring antibiotic resistance genes, antibiotic inactivation genes, and antibiotic target alteration genes were also identified. The results expand scientific understanding on how *Salmonella* isolates with high biofilm-forming capacity and multidrug resistance survive in stressful conditions in the industry.

Keywords: biofilm; genome sequencing; multidrug resistance; *Salmonella* Typhimurium

Introduction

Salmonella Typhimurium is one of the major zoonotic bacteria that can cause serious gastroenteritis, typhoid fever, diarrhea, and sepsis (Taylor and Winter, 2020). This bacterium is usually transmitted to humans via the consumption of poultry products, or sometimes by contaminated surfaces (Shen *et al.*, 2022). Although Chinese official data for *Salmonella* contamination in foods is not available, many studies have indicated that the prevalence of *Salmonella* was found to be 10.7–71.8%, with

S. Typhimurium being one of the most predominant serovars (Zhou *et al.*, 2018). In addition, studies have declared that the major concerns of *S. Typhimurium* in the food industry are the ability to acquire antimicrobial resistance and form biofilms on surfaces (Merino *et al.*, 2019; Wang *et al.*, 2022).

Antibiotics are used to both control the animal infections caused by *Salmonella*, and alleviate the widespread of salmonellosis among humans. Unfortunately, with the overuse of antibiotics in agriculture, *S. Typhimurium*

is becoming highly resistant to a variety of antibiotics including lincomycin, tetracycline, quinolones, sulfamethoxazole, and oxytetracycline (Ingle *et al.*, 2021; Tian *et al.*, 2021). The occurrence of multidrug-resistant *S. Typhimurium* could cause treatment failure in animal husbandry and constitute huge threats to public health.

Biofilm formation has been proved to be a key factor that contributes to the ineffectiveness of antibiotics, which allows for the persistence of *S. Typhimurium* in the food industry (Yuan *et al.*, 2021). Defined as the assemblage of microbes within the self-produced extracellular polymeric substances (EPS), biofilms are a regular mode for bacterial growth in nature, which account for around 80% of bacterial infections globally (Yuan *et al.*, 2020). Many studies have indicated the occurrence of *S. Typhimurium* on meat products, glasses, plastics, stainless steel, and rubber in poultry processing environments, and the presence in the above environs is strongly linked to its biofilm-forming capacity (Lee *et al.*, 2020). Once formed, *S. Typhimurium* biofilms are believed to show much higher resistance to antibiotics compared to their free-living counterparts, leading to the continuous transmission of foodborne diseases in the food industry (Yuan *et al.*, 2020).

In this study, the biofilm-forming capacity and antibiotic resistance profiles of *S. Typhimurium* isolates from a swine slaughterhouse were evaluated. In addition, genome sequencing was performed to determine the genes of a unique *S. Typhimurium* isolate with multi-characteristics of high biofilm-forming ability and multidrug resistance. The results could provide new insights into the persistence of *S. Typhimurium* in the food industry, which would be valuable to effectively control *Salmonella* contamination in the food industry.

Materials and Methods

Bacterial strain and culture conditions

In this study, 39 *S. Typhimurium* isolates were isolated from a swine slaughterhouse in Jiangsu, China, from October 2016 to April 2017 (Zhou *et al.*, 2018). The cultures of *S. Typhimurium* were stored at -80°C in tryptic soy broth (TSB, Difco, USA), which contained 20% (v/v) glycerol.

Biofilm formation by *S. Typhimurium*

Biofilm formation by *S. Typhimurium* was determined according to the crystal violet staining assay described by Yuan *et al.* (2018). In brief, aliquots of 200 μL bacterial culture at a concentration of 10^4 CFU/mL in TSB were

added into six wells of a 96-well plate (Costar, Corning, USA). Six negative controls with only TSB were also included. After incubation for 24 h at 37°C , the medium was gently poured, and each well was washed with sterile phosphate buffer saline (PBS), followed by fixing with methanol. Each well was stained by 200 μL of 0.05% (w/v) crystal violet solution (Sigma, USA) for 10 min, and washed with PBS. Adhered crystal violet in each well was then solubilized in 200 μL of 33% (v/v) acetic acid. The microplate reader (Thermo Fisher, USA) was used to measure optical density (OD) of the solution in wells at 594 nm. Biofilm-forming ability of each *S. Typhimurium* isolate was expressed by cut-off OD (OD_c), which was defined as the mean OD of negative control plus three standard deviations (SD). Biofilm-forming capacity of each *S. Typhimurium* isolate was classified as the following groups: strong biofilm former (OD > 4OD_c), moderate biofilm former (4OD_c \geq OD > 2OD_c), weak biofilm former (2OD_c \geq OD > OD_c), and no biofilm former (OD_c \geq OD) (Diaz *et al.*, 2016). All results are expressed as mean \pm SD obtained from assays with three replicates.

Biofilm formation of *S. Typhimurium* isolates on stainless steel surface was measured by following the assay as described by Yuan *et al.* (2018). Stainless steel coupons (with a square size of 1×1 cm) were immersed in acetone, washed with 75% (v/v) ethanol, rinsed with water, and then autoclaved before use. The overnight culture of each *S. Typhimurium* isolate was inoculated in 100 mL TSB in a flask containing coupons to obtain the final bacterial concentration of 10^4 CFU/mL. After the incubation at 37°C for 24 h, stainless steel coupons were removed, washed with sterile PBS (pH 7), and transferred to a tube containing 10 g of glass beads and 10 mL of sterile PBS (pH 7). Adhered cells were detached from stainless steel surface by vortex mixing for 120 s. Each bacterial suspension was decimally diluted and plated onto TSA plates, followed by the incubation for 48 h at 28°C . All results are expressed as mean \pm SD obtained from assays with three replicates.

Antimicrobial resistance of the high-biofilm former *S. Typhimurium* M3

Antibiotic resistance of the high-biofilm former *S. Typhimurium* M3 was assessed based on the diffusion method of Clinical Laboratory Standards Institute (CLSI) guidelines (2016). Commercial antibiotic discs (HiMedia, India) contain 22 antibiotics (Table 1). In brief, 100 μL of overnight *S. Typhimurium* M3 culture was spread onto TSA plates. Then, antibiotic discs were placed on plates, followed by the incubation for 20 h at 37°C . Inhibition zones (mm) were measured and categorized as susceptible (S), intermediate (IR), and resistant (R)

Table 1. Antibiotic susceptibility of *Salmonella* Typhimurium M3.

Antibiotics	Antimicrobial resistance	Antibiotics	Antimicrobial resistance
Oxacillin (1 µg)	R	Doxycycline (30 µg)	I
Amoxicillin (20 µg)	S	Enrofloxacin (10 µg)	S
Gentamicin (10 µg)	I	Azithromycin (15 µg)	I
Streptomycin (10 µg)	I	Norfloxacin (10 µg)	S
Penicillin (10 µg)	S	Lomefloxacin (10 µg)	S
Cefotaxime (30 µg)	S	Nitrofurantoin (300 µg)	S
Cotrimoxazole (1.25 µg)	S	Ampicillin (10 µg)	S
Polymyxin B (10 µg)	I	Rifampicin (5 µg)	R
Amikacin (30 µg)	S	Clindamycin (10 µg)	R
Novobiocin (10 µg)	I	Erythromycin (15 µg)	I
Lincomycin (10 µg)	R	Tetracycline (30 µg)	R

R, Resistant (≤ 14 mm); IR, Intermediate resistant (15–19 mm); S, Susceptible (≥ 20 mm).

according to each zone diameter of ≥ 20 , 15–19, and ≤ 14 mm, respectively.

Defined as the lowest concentration of antibiotics that can inhibit bacterial growth, the MIC of antibiotics in *S. Typhimurium* M3 was assessed by the broth microdilution method (Dawan and Ahn, 2020). In brief, different dilutions of antibiotics and *S. Typhimurium* M3 were inoculated in 96-well plates at 37°C for 24 h.

Genome sequencing of *S. Typhimurium* M3

Genomic DNA of *S. Typhimurium* M3 was extracted by E.Z.N.A.[®] Bacterial DNA Kit (Omega, USA) according to the instructions. DNA quality was assessed by NanoDrop 2000 spectrophotometer (Thermo Fisher Scientific, USA). Preparation for library was performed based on Illumina's TruSeq Nano DNA Sample Prep Kit. Whole genome of *S. Typhimurium* M3 was sequenced by Illumina novaseq 6000 (Illumina Inc, San Diego, USA). Raw paired-end reads were trimmed and filtered using Trimmomatic, and sequences were assembled by ABySS. Genes in the genome of *S. Typhimurium* M3 were predicted with GeneMarkS. All gene models were blastp against nonredundant (NR) database, Kyoto Encyclopedia of Genes and Genomes (KEGG), Gene Ontology (GO),

and Cluster of Orthologous Group (COG) for functional annotation. A circular map of *S. Typhimurium* M3 genome was drawn using Circos. Antibiotic resistance genes in the *S. Typhimurium* M3 genome were predicted by Resistance Gene Identifier against the Comprehensive Antibiotic Resistance Database (CARD).

Results and Discussion

Biofilm formation by *S. Typhimurium* isolates

Biofilm formation by *S. Typhimurium* in food industry may cause huge economic losses and serious safety issues globally. In this study, the biofilm-forming capacity of each *S. Typhimurium* isolate was quantified by the crystal violet staining assay. The OD₅₉₄ values of *S. Typhimurium* isolates ranged from 0.017 to 1.098, and the highest OD₅₉₄ value was obtained from *S. Typhimurium* M3. Biofilm-forming ability was proved to be in a strain-dependent way, as 9, 12, and 18 isolates were classified as weak, moderate, and strong biofilm formers, respectively (Figure 1A). High biofilm-forming ability of *S. Typhimurium* was also observed in previous studies, providing them survival strategies against antibiotics (Lee *et al.*, 2020). Characteristics of different food-contact surfaces could influence bacterial attachment and biofilm formation of microorganisms. In this work, isolates belonging to *S. Typhimurium* were also measured for their biofilm-forming capacity on stainless steel surface to simulate the real situation in the food industry. Cell counts recovered from biofilms of all *S. Typhimurium* isolates were in a range from 2.96 to 8.06 log CFU/cm² (Figure 1B). High biofilm-forming capacity (7.95 log CFU/cm²) of *S. Typhimurium* M3 on stainless steel coupon was also found. A previous study proved that *Salmonella* could be transferred from biofilms formed on stainless steel coupons to poultry products, posing safety issues to consumers (Wang *et al.*, 2015). Therefore, the high biofilm-forming ability of *S. Typhimurium* observed in this study indicates the need to optimize the cleaning and disinfection procedures to avoid *Salmonella* biofilm contamination.

Antibiotic resistance of *S. Typhimurium* M3

The wide spread of multidrug-resistant *Salmonella* has made it a threat to public health. The high biofilm-forming isolate *S. Typhimurium* M3 was selected to test its susceptibility to 22 antibiotics by the diffusion method (Table 1). *S. Typhimurium* M3 was resistant to oxacillin, lincomycin, rifampicin, tetracycline, and clindamycin, and intermediate resistant to gentamicin, streptomycin, polymyxin B, novobiocin, doxycycline, azithromycin, and erythromycin. Furthermore, the MICs

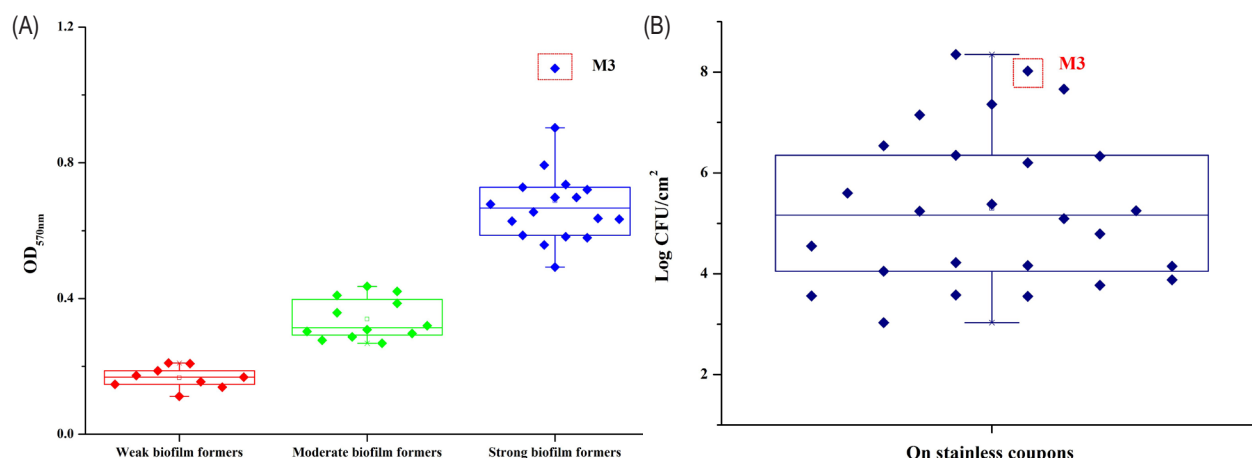


Figure 1. Biofilm formation of 39 *Salmonella Typhimurium* isolates on both polystyrene (A) and stainless steel coupons (B).

of oxacillin, lincomycin, rifampicin, tetracycline, and clindamycin were 512, 32, 16, 64, and 64 ug/mL, respectively. Occurrence of resistance to these antibiotics of *S. Typhimurium* have already been proved in different countries (Dawan and Ahn, 2020; Harb *et al.*, 2018). It is speculated that the resistance to multiple antibiotics may be caused by several mechanisms, including altering the cell membrane permeability, modifying the site of drug action, interfering with DNA synthesis, and affecting the structure of cell wall (Enrique *et al.*, 2020).

Genome properties of *S. Typhimurium* M3

This work also aims to determine the genome properties of *S. Typhimurium* M3 with unique multi-characteristics of high biofilm-forming and multidrug resistance. The draft genome sequence of *S. Typhimurium* M3 had a length of 4881503 bp, a GC content of 52.17%, which contained 4579 coding sequences, 81 tRNAs, 8 rRNAs (6 of 5S rRNA, 1 of 16S rRNA, and 1 of 23S rRNA) (Table 2). The circular representation of *S. Typhimurium* M3 draft genome is shown in Figure 2.

The proteins with functional assignments of *S. Typhimurium* M3 included 2276 with GO assignments,

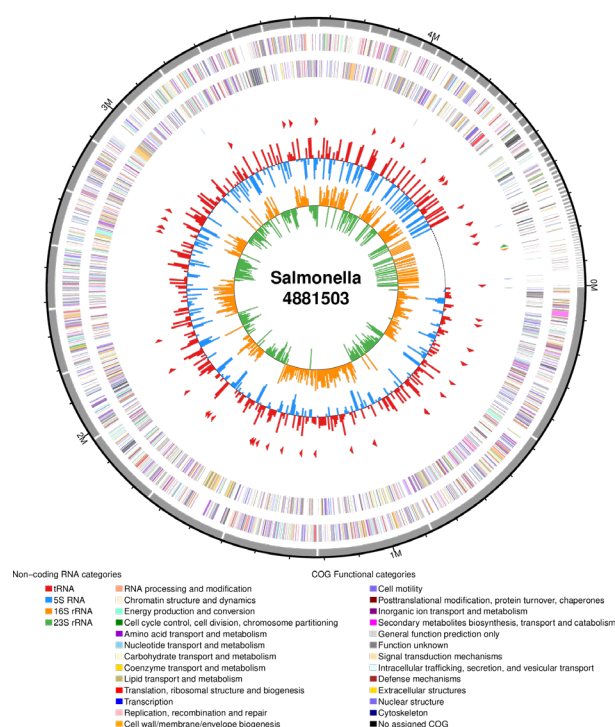


Figure 2. Genomic circle map of *Salmonella Typhimurium* M3.

3882 with eggNOG, 138 with CARD, and 3171 with KEGG pathway mapping. The COG protein database was generated by the comparison of predicted and known proteins in completely sequenced microbial genomes to infer sets of orthologs (Figure 3). In this study, the COG annotation showed that transcription, carbohydrate transport and metabolism, energy production and conversion, and amino acid transport and metabolism were the most abundant categories. Furthermore, KEGG annotation showed that 2003, 485, 263, and 245 genes were participated in overview maps, carbohydrate metabolism, amino acid metabolism, and membrane transport, respectively (Figure 4).

Table 2. Genome properties of *Salmonella Typhimurium* M3.

Attributes	<i>Salmonella Typhimurium</i> M3
Genome size	4881503 bp
Protein coding genes	4579
G-C content	52.17%
rRNA encoding genes	8
tRNA encoding genes	81
Total scaffolds	80
Scaffold N50	208949 bp
Scaffold N90	47339 bp

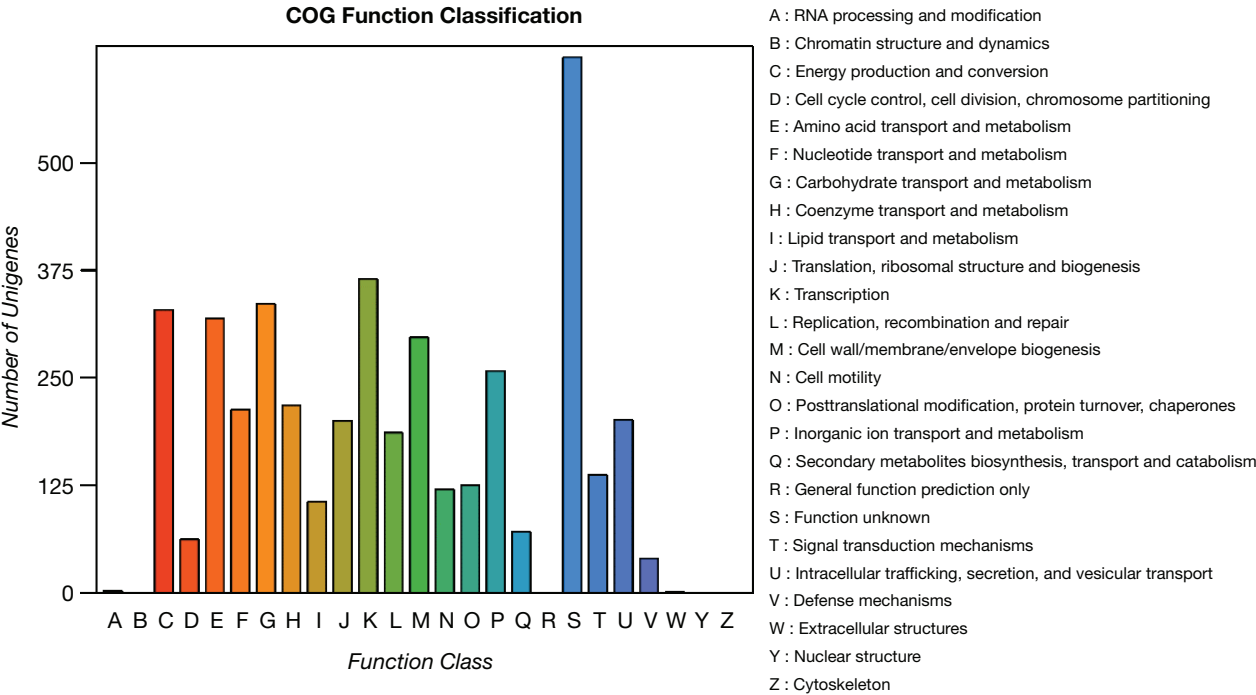


Figure 3. Cluster of orthologous group annotation of genes in *Salmonella Typhimurium* M3.

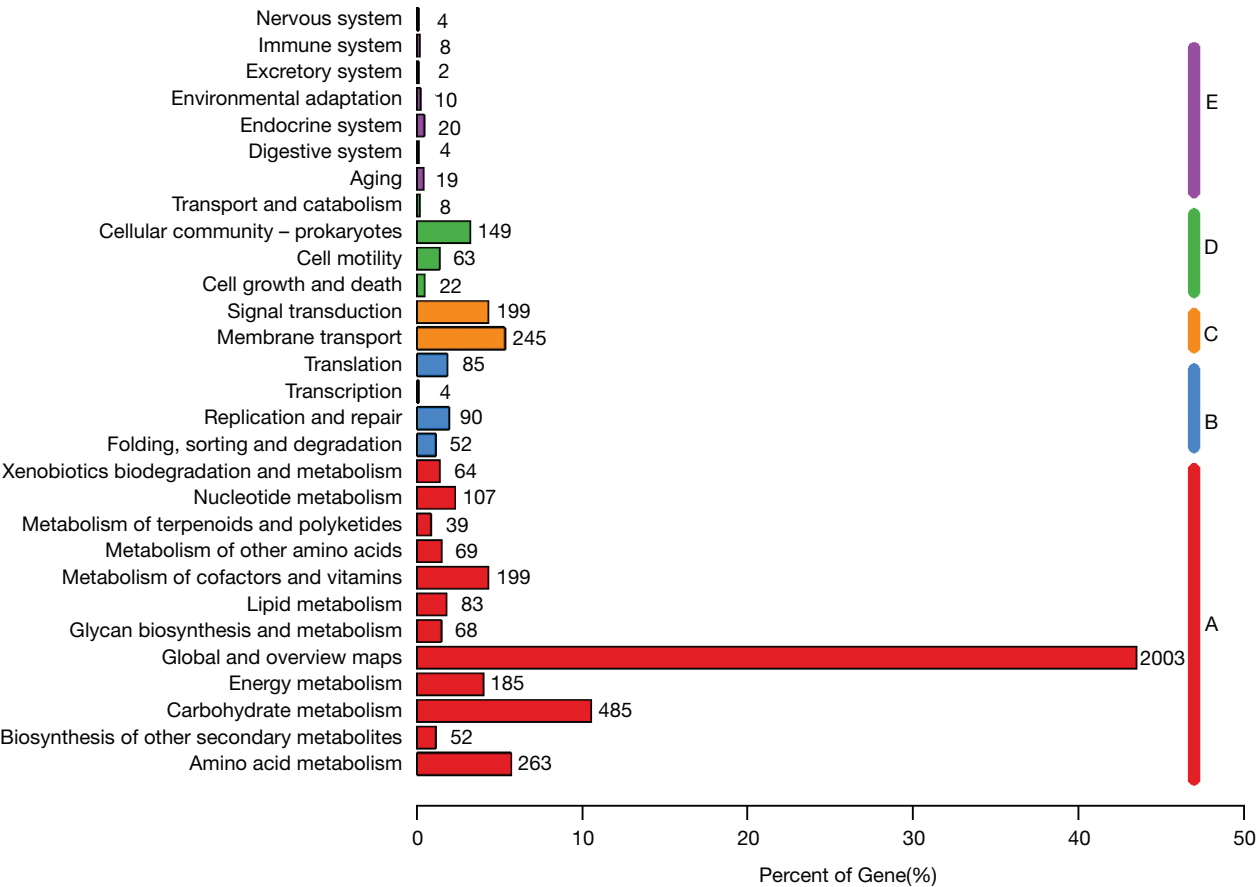


Figure 4. Kyoto encyclopedia of genes and genomes pathway enrichment results of genes in *Salmonella Typhimurium* M3.

The genome analysis of *S. Typhimurium* M3 showed several genes related to antibiotic resistance by antibiotic efflux, antibiotic target alteration, and antibiotic inactivation (Table 3). Antimicrobial resistance genes were predicted based on the CARD database, and

Table 3. Genes essential for antibiotic resistance in genome of *Salmonella* Typhimurium M3.

Gene identified	General function	Resistance mechanism
<i>aac6-I</i>	Cryptic aminoglycoside N-acetyltransferase AAC(6')-ly/Iaa	Antibiotic inactivation
<i>acrA</i>	Multidrug efflux RND transporter periplasmic adaptor subunit AcrA	Antibiotic efflux
<i>acrB</i>	Multidrug efflux pump subunit AcrB	Antibiotic efflux
<i>acrD</i>	Multidrug efflux RND transporter permease AcrD	Antibiotic efflux
<i>acrE</i>	Efflux RND transporter periplasmic adaptor subunit	Antibiotic efflux
<i>acrF</i>	Multidrug efflux RND transporter permease subunit	Antibiotic efflux
<i>acrR</i>	Multidrug efflux transporter transcriptional repressor AcrR	Antibiotic efflux
<i>ampH</i>	D-alanyl-D-alanine-carboxypeptidase/endopeptidase AmpH	Antibiotic inactivation
<i>baeR</i>	Two-component system response regulator BaeR	Antibiotic efflux
<i>baeS</i>	Two-component system sensor histidine kinase BaeS	Antibiotic efflux
<i>cpxA</i>	Envelope stress sensor histidine kinase CpxA	Antibiotic efflux
<i>crp</i>	cAMP-activated global transcriptional regulator CRP	Antibiotic efflux
<i>cyaA</i>	Adenylate cyclase	Antibiotic target alteration
<i>emrA</i>	Multidrug efflux MFS transporter periplasmic adaptor subunit EmrA	Antibiotic efflux
<i>emrB</i>	Inner membrane component of tripartite multidrug resistance system	Antibiotic efflux
<i>emrR</i>	Transcriptional repressor MprA	Antibiotic efflux
<i>fabI</i>	Enoyl-ACP reductase FabI	Antibiotic target alteration
<i>folP</i>	Dihydropteroate synthase	Antibiotic target alteration
<i>glpT</i>	Glycerol-3-phosphate transporter	Antibiotic target alteration
<i>golS</i>	MerR family transcriptional regulator	Antibiotic efflux
<i>gyrA</i>	DNA gyrase subunit A	Antibiotic target alteration
<i>gyrB</i>	DNA gyrase subunit B	Antibiotic target alteration
<i>hns</i>	DNA-binding transcriptional regulator H-NS	Antibiotic efflux
<i>kdpE</i>	Two-component system response regulator KdpE	Antibiotic efflux

(Continues)

Table 3. Continued.

Gene identified	General function	Resistance mechanism
<i>marA</i>	MDR efflux pump AcrAB transcriptional activator MarA	Antibiotic efflux
<i>marR</i>	Multiple antibiotic resistance protein MarR	Antibiotic efflux
<i>mdtA</i>	Multidrug resistance protein MdtA	Antibiotic efflux
<i>mdtB</i>	Multidrug resistance protein MdtB	Antibiotic efflux
<i>mdtC</i>	Multidrug efflux RND transporter permease subunit MdtC	Antibiotic efflux
<i>mdtG</i>	Multidrug efflux MFS transporter MdtG	Antibiotic efflux
<i>mdtH</i>	Multidrug efflux MFS transporter MdtH	Antibiotic efflux
<i>mdtK</i>	Multidrug efflux MATE transporter MdtK	Antibiotic efflux
<i>mdtM</i>	Multidrug resistance protein MdtM	Antibiotic efflux
<i>mdsA</i>	Multidrug efflux RND transporter periplasmic adaptor subunit MdsA	Antibiotic efflux
<i>mdsB</i>	Multidrug efflux RND transporter permease subunit MdsB	Antibiotic efflux
<i>mdsC</i>	Efflux pump outer membrane protein	Antibiotic efflux
<i>msbA</i>	Lipid A ABC transporter ATP-binding protein/permease MsbA	Antibiotic efflux
<i>murA</i>	UDP-N-acetylglucosamine 1-carboxyvinyltransferase	Antibiotic target alteration
<i>nfsA</i>	Nitroreductase A	Antibiotic target alteration
<i>parC</i>	DNA topoisomerase IV subunit A	Antibiotic target alteration
<i>parE</i>	DNA topoisomerase IV subunit B	Antibiotic target alteration
<i>phoP</i>	Two-component system response regulator PhoP	Antibiotic target alteration
<i>ptsI</i>	Phosphoenolpyruvate-protein phosphotransferase PtsI	Antibiotic target alteration
<i>ramA</i>	RamA family antibiotic efflux transcriptional regulator	Antibiotic efflux
<i>sdiA</i>	Transcriptional regulator SdiA	Antibiotic efflux
<i>rpoB</i>	DNA-directed RNA polymerase subunit beta	Antibiotic target alteration
<i>soxS</i>	Superoxide response transcriptional regulator SoxS	Antibiotic target alteration
<i>soxR</i>	Redox-sensitive transcriptional activator SoxR	Antibiotic target alteration
<i>tetA</i>	Tetracycline resistance protein	Antibiotic efflux
<i>tolC</i>	Outer membrane channel protein TolC	Antibiotic efflux
<i>tuf</i>	Elongation factor Tu	Antibiotic target alteration
<i>uhpA</i>	DNA-binding transcriptional activator UhpA	Antibiotic target alteration
<i>uhpT</i>	Hexose-6-phosphate:phosphate antiporter	Antibiotic target alteration
<i>yojI</i>	Multidrug ABC transporter permease/ATP-binding protein	Antibiotic efflux

S. Typhimurium M3 contained 18 genes connected with resistance to tetracycline (*tetA*), fluoroquinolone (*gyrB*, *parC*, *parE*), triclosan (*gyrA*), sulfonamide (*folP*), nitrofurantoin (*nfsA*), elfamycin (*tuf*), aminoglycoside (*AAC6*), rifamycin (*rpoB*), fosfomycin (*uhpA*, *uhpT*, *ptsI*, *murA*, *cyaA*, *glpT*), cephalosporin (*ampH*), and isoniazid (*fabI*). Remarkably, in this study, 36 genes belonged to several gene families, including ATP-binding cassette (ABC) antibiotic efflux pumps (*soxS*, *soxR*, *phoP*, *msbA*, *tolC*, *yojI*), resistance-nodulation–cell division (RND) antibiotic efflux pumps (*acrA*, *acrE*, *acrR*, *baeR*, *baeS*, *cpxA*, *golS*, *marR*, *mdsA*, *mdsB*, *mdsC*, *sdiA*, *crp*, *marA*, *acrB*, *acrD*, *acrF*, *mdtA*, *mdtB*, *mdtC*, *ramA*), major facilitator superfamily (*emrA*, *emrB*, *emrR*, *hns*, *mdtG*, *mdtH*, *mdtM*), multidrug and toxic compound extrusion (MATE) transporters (*mdtK*), and KdpDE (*kdpE*) identified in the genome of *S. Typhimurium* M3. The presence of efflux pumps makes *S. Typhimurium* isolates insensitive to tetracycline, oxacillin, lincomycin, rifampicin, streptomycin, clindamycin, kanamycin, ciprofloxacin, norfloxacin (Ge et al., 2022; Zwama and Nishino, 2021).

In this study, key genes encoding for chemotaxis, motility, surface attachment, quorum sensing (QS), matrix protein-encoding genes, biofilm transcriptional regulators, and matrix polysaccharide synthesis genes were also identified (Table 4). Some of the adhesion factors, such

Table 4. Genes essential for biofilm formation in the genome of *Salmonella Typhimurium* M3.

Gene identified	General function	Biofilm regulation mechanism
<i>cheV</i>	Involved in the transmission of sensory signals from the chemoreceptors to the flagellar motors	Chemotaxis
<i>luxS</i>	S-ribosylhomocysteine lyase	Quorum sensing
<i>flgA</i>	Flagellar basal body P-ring formation protein FlgA	Flagellar
<i>flgB</i>	Flagellar basal body rod protein FlgB	Flagellar
<i>flgC</i>	Flagellar basal body rod protein FlgC	Flagellar
<i>flgD</i>	Flagellar hook assembly protein FlgD	Flagellar
<i>flgE</i>	Flagellar hook protein FlgE	Flagellar
<i>flgF</i>	Flagellar basal body rod protein FlgF	Flagellar
<i>flgG</i>	Flagellar basal body rod protein FlgG	Flagellar
<i>flgH</i>	Flagellar basal body L-ring protein FlgH	Flagellar
<i>flgI</i>	Flagellar basal body P-ring protein FlgI	Flagellar

(Continues)

Table 4. Continued.

Gene identified	General function	Biofilm regulation mechanism
<i>flgJ</i>	Flagellar assembly peptidoglycan hydrolase FlgJ	Flagellar
<i>flgK</i>	Flagellar hook-associated protein FlgK	Flagellar
<i>flgL</i>	Flagellar basal body-associated protein FlgL	Flagellar
<i>flgM</i>	Flagellar motor switch protein FlgM	Flagellar
<i>flgN</i>	Flagellar motor switch protein FlgN	Flagellar
<i>flgO</i>	Flagellar type III secretion system protein FlgO	Flagellar
<i>flgP</i>	Flagellar type III secretion system pore protein FlgP	Flagellar
<i>flgQ</i>	Flagellar biosynthesis protein FlgQ	Flagellar
<i>bcsA</i>	UDP-forming cellulose synthase catalytic subunit	Cellulose biosynthesis
<i>bcsB</i>	Cellulose biosynthesis cyclic di-GMP-binding regulatory protein BcsB	Cellulose biosynthesis
<i>bcsC</i>	Cellulose biosynthesis protein BcsC	Cellulose biosynthesis
<i>bcsE</i>	Cellulose biosynthesis protein BcsE	Cellulose biosynthesis
<i>bcsF</i>	Cellulose biosynthesis protein BcsF	Cellulose biosynthesis
<i>bcsG</i>	Cellulose biosynthesis protein BcsG	Cellulose biosynthesis
<i>bcsQ</i>	Cellulose biosynthesis protein BcsQ	Cellulose biosynthesis
<i>csgA</i>	Major curlin subunit	Curli production
<i>csgB</i>	Minor curlin subunit	Curli production
<i>csgE</i>	Curli production assembly/transport protein CsgE	Curli production
<i>csgF</i>	Curli production assembly/transport protein CsgF	Curli production
<i>csgG</i>	Curli production assembly/transport protein CsgG	Curli production
<i>fimA</i>	Type-1 fimbrial protein subunit	Biogenesis of fimbriae
<i>fimC</i>	Fimbrial chaperone protein FimC	Biogenesis of fimbriae
<i>fimF</i>	Fimbrial-like protein FimF	Biogenesis of fimbriae
<i>fimH</i>	Fimbrial protein FimH	Biogenesis of fimbriae
<i>fimW</i>	Fimbria biosynthesis transcriptional regulator FimW	Biogenesis of fimbriae
<i>fimY</i>	Fimbria biosynthesis regulator FimY	Biogenesis of fimbriae
<i>lpfB</i>	Fimbrial assembly chaperone	Biogenesis of fimbriae
<i>yhcD</i>	Fimbrial biogenesis outer membrane usher protein	Biogenesis of fimbriae

(Continues)

Table 4. Continued.

Gene identified	General function	Biofilm regulation mechanism
<i>yhcA</i>	Fimbrial chaperone protein	Biogenesis of fimbriae
<i>mrkB</i>	Fimbrial assembly chaperone	Biogenesis of fimbriae
<i>csgD</i>	Transcriptional regulator CsgD	Transcriptional regulator
<i>adrA</i>	Diguanylate cyclase AdrA	Transcriptional regulator
<i>sdiA</i>	transcriptional regulator SdiA	Transcriptional regulator
<i>flk</i>	Flagella biosynthesis regulator Flk	Flagellar regulator
<i>bapA</i>	Biofilm-associated protein BapA	Cell-surface protein
<i>bssS</i>	Biofilm formation regulatory protein BssS	Biofilm regulator
<i>bsmA</i>	Lipoprotein BsmA	Biofilm stress and motility protein
<i>bdcA</i>	SDR family oxidoreductase	Increases biofilm dispersal
<i>yehA</i>	Putative fimbrial-like adhesin protein	Contributes to adhesion to various surfaces in specific environmental niches

as flagella and pili, are vital for biofilm formation (Yuan *et al.*, 2020). Genes related to flagellar (*flgA*, *flgB*, *flgC*, *flgD*, *flgE*, *flgF*, *flgG*, *flgH*, *flgI*, *flgJ*, *flgK*, *flgL*, *flgM*, *flgN*, *flgO*, *flgP*) identified in this study are essential for attachment but can serve different roles during *Salmonella* biofilm formation. Gene coding for chemotaxis (*cheV*) in this study is involved in the transmission of sensory signals from the chemoreceptors to the flagellar motors. QS is the bacterial cell-to-cell communication signaling mechanism, which can regulate bacterial motility and biofilm formation (Yuan *et al.*, 2018). The *luxS* gene detected in this study is responsible for the production of QS signaling molecule by converting S-ribosyl-L-homocysteine into homocysteine and DPD. EPS of *S. Typhimurium* biofilms is composed of cellulose, curli, and biofilm-associated protein, and can support the adherence and surface attachment of *S. Typhimurium* onto different surfaces (Maruzani *et al.*, 2019). In this study, the genes for cellulose biosynthesis (*bcsA*, *bcsB*, *bcsC*, *bcsE*, *bcsF*, *bcsG*, *bcsQ*), curli production (*csgA*, *csgB*, *csgE*, *csgF*, *csgG*), fimbriae biogenesis (*fimA*, *fimC*, *fimF*, *fimH*, *fimW*, *fimY*, *lpfB*, *yhcD*, *yhcA*, *mrkB*) were identified. Biofilm formation by *Salmonella* has proved to be regulated by a complex genetic network involving interactions between

regulators, and the major regulators including *csgD*, *adrA*, and *flk* were identified in this study. CsgD encoded by *csgD* is the biofilm control center to regulate expressions of major *Salmonella* biofilm constituents, control the transition between planktonic and biofilm cells, and even maintain the 3-D structure of biofilms (Chen *et al.*, 2021). AdrA regulates genes encoding cellulose biosynthesis of *Salmonella* by changing cellular levels of c-di-GMP during biofilm formation (Chen *et al.*, 2021). The large protein BapA (encoded by *bapA*) of *S. Typhimurium* was shown to be necessary for bacterial aggregation and pellicle formation by interconnecting individual cells.

Conclusion

In summary, the high biofilm-forming capacity and multi-drug resistance of *S. Typhimurium* from swine slaughterhouse evidenced by *in vitro* and genomic sequencing tests confirmed their persistence in the food industry. The results have significant implications for the food safety and public health globally, highlighting the importance of good hygienic practices and appropriate use of antibiotics in the industry. Furthermore, the development of more appropriate and effective approaches for control of *Salmonella* contamination control in the food industry are also critical.

Acknowledgments

This research was financially supported by the Natural Science Fund for Colleges and Universities in Jiangsu Province (21KJB550007), the Natural Science Foundation of Jiangsu Province (BK20210814), and China Postdoctoral Science Foundation (2021TQ0274, 2022M720120).

References

- Chen, S., Feng, Z., Sun, H., Zhang, R., Qin, T. and Peng, D., 2021. Biofilm-formation-related genes *csgD* and *bcsA* promote the vertical transmission of *Salmonella* Enteritidis in Chicken. *Frontiers in Veterinary Science* 7: 625049. <https://doi.org/10.3389/fvets.2020.625049>
- CLSI (Clinical and Laboratory Standard Institute), 2016. Performance standards for antimicrobial susceptibility testing. Twenty-Second Informational Supplement.
- Dawan, J. and Ahn, J., 2020. Assessment of cross-resistance potential to serial antibiotic treatments in antibiotic-resistant *Salmonella* Typhimurium. *Microbial Pathogenesis* 148: 104478. <https://doi.org/10.1016/j.micpath.2020.104478>
- Diaz, M., Ladero, V., Rio, B.D., Redruello, B., Fernandez, M., Martin, M.C. and Alvarez, M.A., 2016. Biofilm-forming capacity in biogenic amine-producing bacteria isolated from dairy

- products. *Frontiers in Microbiology* 7: 591. <https://doi.org/10.3389/fmicb.2016.00591>
- Enrique Castro-Vargas, R.E., Herrera-Sanchez, M.P., Rodriguez-Hernandez, R. and Rondon-Barragan, I.S., 2020. Antibiotic resistance in *Salmonella* spp. isolated from poultry: a global overview. *Veterinary World* 13: 2070–2084. <https://doi.org/10.14202/vetworld.2020.2070-2084>
- Ge, H.W., Wang, Y.Z. and Zhao, X.H., 2022. Research on the drug resistance mechanism of foodborne pathogens. *Microbial Pathogenesis* 162: 105306. <https://doi.org/10.1016/j.micpath.2021.105306>
- Harb, A., Habib, I., Mezal, E.H., Kareem, H.S., Laird, T., O'Dea, M. and Abraham, S., 2018. Occurrence, antimicrobial resistance and whole-genome sequencing analysis of *Salmonella* isolates from chicken carcasses imported into Iraq from four different countries. *International Journal of Food Microbiology* 284: 84–90. <https://doi.org/10.1016/j.ijfoodmicro.2018.07.007>
- Ingle, D.J., Ambrose, R.L., Baines, S.L., Duchene, S., da Silva, A.G., Lee, D.Y.J., Jones, M., Valcanis, M., Taiaroa, G. and Ballard, S.A., 2021. Evolutionary dynamics of multidrug resistant *Salmonella enterica* serovar 4,[5],12:i:- in Australia. *Nature Communications* 12: 4786. <https://doi.org/10.1038/s41467-021-25073-w>
- Lee, K.H., Lee, J.Y., Roy, P.K., Mizan, M.F.R., Hossain, M.I., Park, S.H. and Ha, S.D., 2020. Viability of *Salmonella* Typhimurium biofilms on major food-contact surfaces and eggshell treated during 35 days with and without water storage at room temperature. *Poultry Science* 99: 4558–4565. <https://doi.org/10.1016/j.psj.2020.05.055>
- Maruzani, R., Sutton, G., Nocerino, P. and Marvasi, M., 2019. Exopolymeric substances (EPS) from *Salmonella enterica*: polymers, proteins and their interactions with plants and abiotic surfaces. *Journal of Microbiology* 57: 1–8. <https://doi.org/10.1007/s12275-019-8353-y>
- Merino, L., Procura, E., Trejo, F.M., Bueno, D.J. and Golowczyc, M.A., 2019. Biofilm formation by *Salmonella* sp. in the poultry industry: detection, control and eradication strategies. *Food Research International* 119: 530–540. <https://doi.org/10.1016/j.foodres.2017.11.024>
- Shen, W.W., Chen, H., Geng, J.W., Wu, R.A., Wang, X. and Ding, T., 2022. Prevalence, serovar distribution, and antibiotic resistance of *Salmonella* spp. isolated from pork in China: a systematic review and meta-analysis. *International Journal of Food Microbiology* 361: 109473. <https://doi.org/10.1016/j.ijfoodmicro.2021.109473>
- Taylor, S.J. and Winter, S.E., 2020. *Salmonella* finds a way: metabolic versatility of *Salmonella enterica* serovar Typhimurium in diverse host environments. *PLoS Pathogens* 16: e1008540. <https://doi.org/10.1371/journal.ppat.1008540>
- Tian, Y., Gu, D., Wang, F., Liu, B., Li, J., Kang, X., Meng, C., Jiao, X.N. and Pan, Z.M., 2021. Prevalence and characteristics of *Salmonella* spp. from a pig farm in Shanghai, China. *Foodborne Pathogens and Disease* 18: 477–488. <https://doi.org/10.1089/fpd.2021.0018>
- Wang, H., Zhang, X., Zhang, Q., Ye, K., Xu, X. and Zhou, G., 2015. Comparison of microbial transfer rates from *Salmonella* spp. biofilm growth on stainless steel to selected processed and raw meat. *Food Control* 50: 574–580. <https://doi.org/10.1016/j.foodcont.2014.09.049>
- Wang, Y.Z., Ge, H.W., Wei, W.Y. and Zhao, X.H., 2022. Research progress on antibiotic resistance of *Salmonella*. *Food Quality and Safety* 6: fyac035. <https://doi.org/10.1093/fqsafe/fyac035>
- Yuan, L., Burmølle, M., Sadiq, F.A., Wang, N. and He, G., 2018a. Interspecies variation in biofilm-forming capacity of psychrotrophic bacterial isolates from Chinese raw milk. *Food Control* 91: 47–57. <https://doi.org/10.1016/j.foodcont.2018.03.026>
- Yuan, L., Hansen, M.F., Røder, H.L., Wang, N., Burmølle, M. and He, G., 2020. Mixed-species biofilms in the food industry: current knowledge and novel control strategies. *Critical Reviews in Food Science and Nutrition* 60: 2277–2293. <https://doi.org/10.1080/10408398.2019.1632790>
- Yuan, L., Sadiq, F.A., Burmølle, M., Liu, T. and He, G., 2018b. Insights into bacterial milk spoilage with particular emphasis on the roles of heat-stable enzymes, biofilms, and quorum sensing. *Journal of Food Protection* 81: 1651–1660. <https://doi.org/10.4315/0362-028X.JFP-18-094>
- Yuan, L., Sadiq, F.A., Wang, N., Yang, Z. and He, G., 2021. Recent advances in understanding the control of disinfectant-resistant biofilms by hurdle technology in the food industry. *Critical Reviews in Food Science and Nutrition* 61: 3876–3891. <https://doi.org/10.1080/10408398.2020.1809345>
- Zhou, Z., Jin, X., Zheng, H., Li, J., Meng, C., Yin, K., Xie, X.L., Huang, C.Y., Lei, T.Y., Sun, X.Y., Xia, Z.M., Zeng, Y., Pan, Z.M. and Jiao, X.N., 2018. The prevalence and load of *Salmonella*, and key risk points of *Salmonella* contamination in a swine slaughterhouse in Jiangsu province, China. *Food Control* 87: 153–160. <https://doi.org/10.1016/j.foodcont.2017.12.026>
- Zwama, M. and Nishino, K., 2021. Ever-adapting RND efflux pumps in Gram-negative multidrug-resistant pathogens: a race against time. *Antibiotics* 10: 774. <https://doi.org/10.3390/antibiotics10070774>